Spin-helicity-dependent magnetic domain growth in a spin-driven multiferroic under applied electric field

Taro Nakajima,* Setsuo Mitsuda, Keiichiro Takahashi, Hiroe Yamazaki, and Keisuke Yoshitomi
Department of Physics, Faculty of Science, Tokyo University of Science, Tokyo 162-8601, Japan

Minoru Soda, Masato Matsuura, and Kazuma Hirota
Department of Earth and Space Science, Graduate School of Science, Osaka University, Osaka 560-8531, Japan
(Received 12 June 2010; revised manuscript received 2 August 2010; published 17 August 2010)

The effects of poling electric field on sizes of magnetic domains have been investigated for a spin-driven multiferroic $CuFe_{1-x}Al_xO_2$, whose ferroelectricity is driven by a screw-type magnetic ordering. By means of polarized neutron-diffraction measurements, we have demonstrated that the application of the electric field on cooling results in differences not only in volume fraction between the right-handed- and the left-handed-helical magnetic domains but also in average size between them. This indicates that on the ferroelectric transition, the electric field accelerates growth of the magnetic domains having ferroelectric polarization parallel to the electric field and suppresses the other.

DOI: 10.1103/PhysRevB.82.064418 PACS number(s): 75.85.+t, 61.05.fm, 75.25.−j

I. INTRODUCTION

"Spin-driven" magnetoelectric (ME) multiferroics, in which magnetic inversion symmetry breaking triggers off ferroelectricity, have been intensively investigated in the recent condensed matter physics research.[1–3] Although the microscopic origins of the spin-driven ferroelectricity are attributed to the local arrangements of the spins, bulk ferroelectric polarization depends on multiferroic domain structures, i.e., sizes, shapes and orientations of the multiferroic domains. Recent studies on several spin-driven multiferroics, such as $ZnCr_2Se_4$ (Ref. 4) or $CuFe_{1-x}Ga_xO_2$,[5] have demonstrated that magnetic field dependences of orientations of multiferroic domains result in distinct changes in ferroelectric polarization. Besides the static ME couplings, dynamical ME responses can also arise from magnetic- and electric-field dependences of the multiferroic domain structures; for example, multiferroic-domain-wall motion driven by ac electric fields accounts for the dielectric dispersion of the giant magnetocapacitance in $DyMnO_3$.[6] To comprehensively understand these ME responses in the spin-driven multiferroics, it is therefore necessary to elucidate the magnetic- and electric-field dependences of the multiferroic domain structures as well as those of the magnetic structures. In the present study, we have demonstrated that average size of multiferroic domains varies with poling electric field (E_p) applied on cooling, in a spin-driven multiferroic $CuFe_{1-x}Al_xO_2$ (CFAO) with $x=0.02$.

A trigonal frustrated magnet $CuFeO_2$ (CFO) exhibits spin-driven ferroelectricity in magnetic-field- or nonmagnetic-substitution-induced magnetic phase.[7–11] CFAO($x=0.02$) to be investigated here exhibits the ferroelectric phase below $T_c \sim 7$ K in zero magnetic field.[9] Magnetic structure in the ferroelectric phase is a (elliptic) screw-type magnetic structure whose modulation wave vector is $(q,q,\frac{3}{2})$ with $q=0.202-0.210$.[12] The screw axis of the magnetic structure is parallel to the c-plane projection of the modulation wave vector. In this paper, we refer to this phase as ferroelectric incommensurate-magnetic (FE-ICM) phase. Because of the trigonal symmetry of the crystal structure, this system has three magnetic domains whose wave vectors of $(q,q,\frac{3}{2})$, $(q,-2q,\frac{3}{2})$, and $(-2q,q,\frac{3}{2})$ are crystallographically equivalent to each other. Along our previous work,[12] we refer to the three domains as (110), $(1\bar{2}0)$, and $(\bar{2}10)$ domains [see Fig. 1(c)]. In each of the domains, the ferroelectric polarization emerges along the screw axes, and moreover, the polarity of the ferroelectric polarization is coupled with spin helicity, i.e., left-handed- (LH-) or right-handed- (RH-) helical arrangements of the spins.[12] Therefore, the multiferroic domains in the FE-ICM phase are classified into six types, as shown in Fig. 1(c).

In previous study, we performed unpolarized neutron-diffraction measurements on CFAO ($x=0.02$) with E_p up to 2.2 MV/m applied along [110] axis, in order to investigate E_p dependence of the magnetic domain structure.[13] As a result, we found that the volume fractions of the (110), $(1\bar{2}0)$, and $(\bar{2}10)$ domains does not depend on E_p. This means that the orientations of the multiferroic domains are not affected by E_p up to 2.2 MV/m. On the other hand, we also found that the widths of the magnetic diffraction profiles in the FE-ICM phase depend on E_p. Since the magnetic ground state of CFAO is not a true long-range order but a small-domain state,[12] the changes in the widths of the diffraction profiles mean that the average size of the magnetic domains varies with E_p. Taking account of the one-to-one correspondence between the spin helicity and the polarity of the ferroelectric polarization, it is natural to consider that the application of E_p increases the average size of the magnetic domains having ferroelectric polarization parallel to E_p, and decreases the other. However, the magnetic reflections measured in the unpolarized neutron-diffraction measurements are superpositions of reflections from the RH- and the LH-helical magnetic orderings. In the present study, we have thus performed polarized neutron-diffraction measurement, which enable us to investigate the spin-helicity-dependent magnetic correlation.

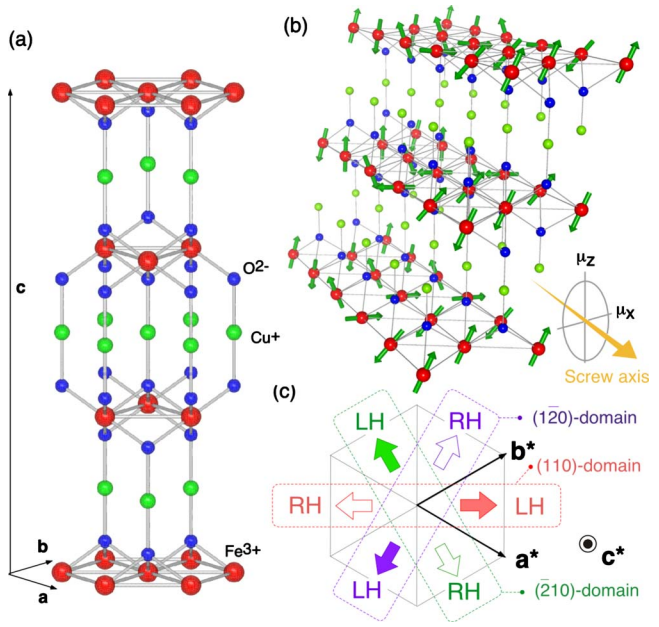

FIG. 1. (Color online) (a) Crystal structure of CFO with a hexagonal basis. (b) The screw-type magnetic structure in the FE-ICM phase. (c) Schematic drawing of the arrangements of the six types of multiferroic domains in the FE-ICM phase. Open and filled arrows denote the directions of the ferroelectric polarization induced by the RH- and the LH-helical magnetic domains.

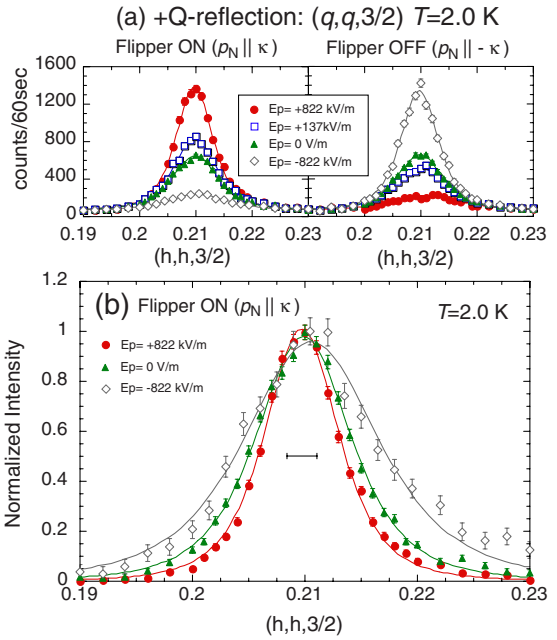

FIG. 2. (Color online) (a) The E_p dependence of the magnetic diffraction profiles measured when the spin flipper is on and off. (b) Comparison of the peak-height-normalized magnetic diffraction profiles measured after cooling with E_p=822,0,−822 kV/m. The effect of imperfect beam polarization has been corrected (Ref. 16). Solid lines are the least-square fits to Lorentzian squared. A horizontal bar represents the experimental resolution limit.

II. EXPERIMENTAL DETAILS

A Single crystal of CFAO(x=0.02) of nominal compositions was prepared by the floating zone method.[14] The polarized neutron-diffraction measurements on CFAO(x=0.02) were carried out at the triple-axis neutron spectrometer PONTA installed by University of Tokyo at JRR-3 in the Japan Atomic Energy Agency. Incident polarized neutron beam with energy 34.05 meV was obtained by a Heusller (111) monochromator. The flipping ratio of the polarized neutron beam was ~17.6. The polarization vector of the incident neutron, $\boldsymbol{p}_N$, was set to be parallel or antiparallel to the scattering vector, $\boldsymbol{\kappa}(=\boldsymbol{k}_i-\boldsymbol{k}_f)$, by a guide field of a helmholtz coil and a spin flipper. The spectrometer was operated in the two-axis mode, and the collimation was open-40′-40′. The sample was cut into a thin plate shape (~3×9×0.8 mm^3) with the flat surfaces normal to the [110] axis, and was mounted in a pumped ^{4}He cryostat with a (h,h,l) scattering plane. The silver paste electrodes were pasted onto the [110] surfaces. Before each measurement, the sample was cooled down from 15 to 2 K under applied E_p.

III. POLARIZED NEUTRON-SCATTERING CROSS SECTIONS

To explore the spin-helicity-dependent magnetic correlation, we start from formulation of polarized neutron-scattering cross section for the screw-type magnetic ordering. In the FE-ICM phase, the system consists of the LH- and the RH-helical magnetic domains. For a moment, we assume that the average sizes of these domains are sufficiently large for the instrumental resolution of the present measurements. Applying the Blume's equation[15] to magnetic reflections belonging to the (110) domain, the scattering cross section is given by

$$\left(\frac{d\sigma}{d\Omega}\right) \propto [F_+V^{\mathrm{LH}}_{(110)} + F_-V^{\mathrm{RH}}_{(110)}]\delta[\boldsymbol{\kappa}-(\boldsymbol{\tau}+\boldsymbol{Q})] + [F_-V^{\mathrm{LH}}_{(110)} + F_+V^{\mathrm{RH}}_{(110)}]\delta[\boldsymbol{\kappa}-(\boldsymbol{\tau}-\boldsymbol{Q})], \quad (1)$$

where $\boldsymbol{Q}=(0.21,0.21,\frac{3}{2})$. $V^{\mathrm{LH}}_{(110)}$ and $V^{\mathrm{RH}}_{(110)}$ are volumes of the LH- and the RH-helical magnetic domains, respectively. $\boldsymbol{\tau}$ is a reciprocal lattice vector. $F_\pm$ is given by $F_\pm=(\mu^2_{x\perp}+\mu^2_{z\perp})\mp 2\mu_{x\perp}\mu_{z\perp}(\boldsymbol{p}_N\cdot\boldsymbol{\kappa}/|\boldsymbol{\kappa}|)$, using lengths of the spin components projected onto the plane normal to the scattering vector, $\mu_{x\perp}$ and $\mu_{z\perp}$, which are defined in the same manner as Ref. 12.

In case that the magnetic domains are relatively small, the δ functions in Eq. (1) are replaced by scattering functions having finite widths in the reciprocal lattice space. For a magnetic reflection located at $\boldsymbol{\tau}+\mathbf{Q}$, where the condition of $(\mu^2_{x\perp}+\mu^2_{z\perp})/2\mu_{x\perp}\mu_{z\perp}\simeq 1$ is satisfied, Eq. (1) can be rewritten as

$$\left(\frac{d\sigma}{d\Omega}\right) \propto S^{\mathrm{LH/RH}}_{(110)}(\boldsymbol{\kappa}), \quad (\pm\mathbf{p}_N \parallel \boldsymbol{\kappa}), \quad (2)$$

where superscripts of "LH" and "RH" correspond to "+" and "−" signs of $\boldsymbol{p}_N$, respectively. $S^{\mathrm{LH}}_{(110)}(\boldsymbol{\kappa})$ [$S^{\mathrm{RH}}_{(110)}(\boldsymbol{\kappa})$] is the scattering functions for the LH- (RH-) helical magnetic orderings. If the average sizes of the LH- and the RH-helical

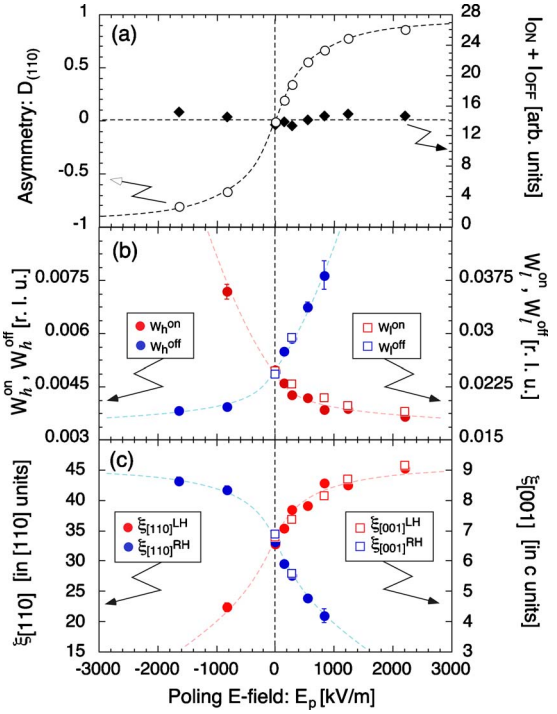

FIG. 3. (Color online) The E_p dependences of (a) $D_{(110)}$ and $I_{ON}+I_{OFF}$, (b) $W_h^{on/off}$ and $W_l^{on/off}$, and (c) $\xi_{[110]}^{LH/RH}$ and $\xi_{[001]}^{LH/RH}$. The dashed lines are guides to eyes.

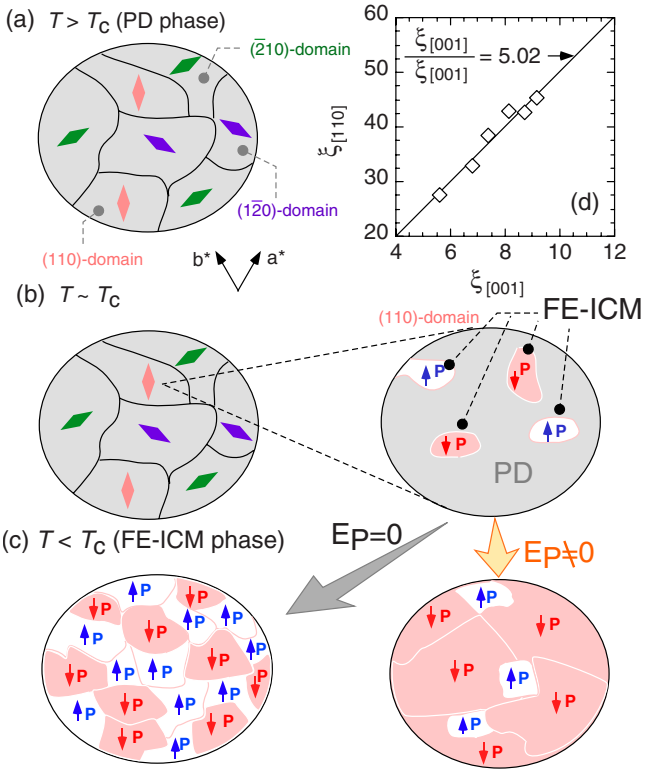

FIG. 4. (Color online) [(a)–(c)] Schematic illustrations of the magnetic phase transitions and the magnetic domain structures in CFAO. Pink, green, and purple lozenges represent the directions of the magnetic modulation wave vectors in the PD phase. (d) The relationship between $\xi_{[110]}$ and $\xi_{[001]}$ obtained in the present measurements.

magnetic domains are different from each other, $S_{(110)}^{LH}(\boldsymbol{\kappa})$ and $S_{(110)}^{RH}(\boldsymbol{\kappa})$ should have different widths in the reciprocal lattice space. Therefore, we can independently deduce the average sizes of the LH- and the RH-helical magnetic domains from the diffraction profiles measured when the spin flipper is on ($\boldsymbol{p}_N \| \boldsymbol{\kappa}$) and off ($-\boldsymbol{p}_N \| \boldsymbol{\kappa}$), respectively.

A ratio between $V_{(110)}^{LH}$ and $V_{(110)}^{RH}$ is given by

$$\frac{V_{(110)}^{LH}}{V_{(110)}^{RH}} = \frac{\int S_{(110)}^{LH}(\boldsymbol{\kappa})d\boldsymbol{\kappa}}{\int S_{(110)}^{RH}(\boldsymbol{\kappa})d\boldsymbol{\kappa}} = \frac{I_{ON}}{I_{OFF}}, \tag{3}$$

where I_{ON} and I_{OFF} are integrated intensities of the magnetic reflection measured when the spin flipper is on and off, respectively.

IV. RESULTS AND DISCUSSIONS

In the present study, we have measured a magnetic reflection located at $(0,0,0)+\boldsymbol{Q}$, where the condition of $(\mu_{x\perp}^2+\mu_{z\perp}^2)/2\mu_{x\perp}\mu_{z\perp} \simeq 1$ is satisfied.[12] Figure 2(a) shows E_p dependence of the diffraction profiles at $T=2$ K. From these profiles, we have obtained asymmetry between $V_{(110)}^{LH}$ and $V_{(110)}^{RH}$, which is defined as $D_{(110)}=(V_{(110)}^{LH}-V_{(110)}^{RH})/(V_{(110)}^{LH}+V_{(110)}^{RH})$, and $I_{ON}+I_{OFF}(\propto V_{(110)}^{LH}+V_{(110)}^{RH})$ as functions of E_p [see Fig. 3(a)]. These results show that the application of E_p increases the volume fraction of the magnetic domains having the ferroelectric polarization parallel to E_p so as to increase the net ferroelectric polarization, while the total volume of the (110) domain, $V_{(110)}^{LH}+V_{(110)}^{RH}$, is not affected by E_p. This is consistent with the previous results on CFAO.[12,13]

We now focus on the widths of the diffraction profiles. Figure 2(b) shows peak-height-normalized diffraction profiles measured after cooling with $E_p=-822, 0, 822$ kV/m, indicating that the width of the diffraction profile varies with E_p.[17] It should be noted that these diffraction profiles are rather broad as compared to the resolution limit and the line shapes are close to Lorentzian squared, which is characteristic to the random-field domain state.[18] This supports that the system consists of relatively small domains.[12] In Fig. 3(b), we show E_p dependences of the half-width at half maximum (HWHM) of the diffraction profiles measured in the $(h,h,\frac{3}{2})$ reciprocal lattice scans. We refer to the HWHM measured when the spin flipper is on (off) as W_h^{on} (W_h^{off}). With increasing E_p, W_h^{on}, and W_h^{off} monotonically decreases and increases, respectively. Moreover, the E_p dependences of W_h^{on} and W_h^{off} are symmetric with respect to $E_p=0$. We also found that the HWHMs for the $(0.21,0.21,l)$ reciprocal lattice scans, W_l^{on} and W_l^{off}, also show similar E_p dependences as those of $W_h^{on/off}$. We have roughly estimated average lengths of the magnetic domains along [110] direction for the LH- and the RH-helical magnetic domains as

$$\xi_{[110]}^{LH/RH} = (2\pi\sqrt{(W_h^{on/off})^2-(W_h^R)^2})^{-1}, \tag{4}$$

where W_h^R is the HWHM of the resolution function for the $(h,h,\frac{3}{2})$ reciprocal lattice scan, and also estimated $\xi_{[001]}^{LH/RH}$ in

the same manner as $\xi_{[110]}^{\mathrm{LH/RH}}$, as shown in Fig. 3(c). These results have revealed that the application of E_p increases the average size of the magnetic domains having ferroelectric polarization parallel to E_p and decreases the other. Keeping the present results in mind, we have schematically depicted the magnetic domain structures of this system at several temperatures in Figs. 4(a)–4(c). Above T_c, CFAO(x=0.02) exhibits a collinear incommensurate magnetic phase referred to as partially disordered (PD) phase, whose propagation wave vector is $(q_{\mathrm{PD}}, q_{\mathrm{PD}}, \frac{3}{2})$ with $q_{\mathrm{PD}} \sim 0.215$. Since the PD magnetic order does not have ferroelectricity, the external electric field does not affect the domain structure. With decreasing temperature from the PD phase, the system undergoes the ferroelectric transition at T_c. Because the phase transition from the PD phase to the FE-ICM phase is a first-order phase transition,[10] the LH- and the RH-helical magnetic domains randomly show up and start to grow at T_c [see Fig. 4(b)].[16] The present results suggest that the application of E_p accelerates the growth of the magnetic domains having the ferroelectric polarization parallel to E_p and suppresses the other. Consequently, at low temperatures, the average sizes of the LH- and the RH-helical magnetic domains are different from each other.

We also found that the ratio between $\xi_{[110]}$ and $\xi_{[001]}$ is not affected by E_p, as shown in Fig. 4(d). This indicates that although the application of E_p affects the sizes of the magnetic domains, it does not their "shapes." This can be ascribed to the three-dimensional nature of the magnetic interactions in this system.[19,20]

It should be mentioned that in the high E_p region, $\xi_{[110]}$ and $\xi_{[001]}$ tend to saturate at ~45 and ~9, respectively. This implies that there still remain many magnetic domain walls even when the net ferroelectric polarization is maximized. This must be ascribed to the local lattice distortions due to the site-random Al substitution, which randomly lift the local degeneracy in the competing exchange interactions and strongly disturb the coherent magnetic ordering.[10,12]

V. CONCLUSION

In conclusion, we have investigated the poling electric field dependence of the multiferroic domain structure in a spin-driven multiferroic CFAO(x=0.02) by means of the polarized neutron-diffraction measurements. The present results successfully demonstrated that the application of E_p on cooling results in not only the asymmetry between the volume fractions of the LH- and the RH-helical magnetic domains but also the difference between the average sizes of them. This kind of poling electric field dependence of magnetic domain sizes must be common to other "spin-driven" multiferroics[21] but might not be clearly observed in neutron-diffraction measurements in case that the magnetic domains are relatively large.[22–25] The reason why it was clearly observed in the present measurements is that the magnetic correlation in the FE-ICM phase of $CuFe_{1-x}Al_xO_2$ (x=0.02) is originally disturbed by the Al^{3+} substitutions.[12,26] We hope that the present results motivate further investigations of static and dynamical ME responses arising form multiferroic domain structures in the spin-driven multiferroics.

ACKNOWLEDGMENTS

The neutron-diffraction measurements at JRR-3 were carried out along the proposal No. 9534B and partly supported by ISSP of the University of Tokyo. The images of the crystal and magnetic structures in this paper were depicted using the software VESTA (Ref. 27).

*nakajima@nsmsmac4.ph.kagu.tus.ac.jp

[1] T. Kimura, T. Goto, H. Shintani, K. Ishizaka, T. Arima, and Y. Tokura, Nature (London) **426**, 55 (2003).
[2] N. Hur, S. Park, P. A. Sharma, J. S. Ahn, S. Guha, and S.-W. Cheong, Nature (London) **429**, 392 (2004).
[3] M. Fiebig, J. Phys. D **38**, R123 (2005).
[4] H. Murakawa, Y. Onose, K. Ohgushi, S. Ishiwata, and Y. Tokura, J. Phys. Soc. Jpn. **77**, 043709 (2008).
[5] S. Seki, H. Murakawa, Y. Onose, and Y. Tokura, Phys. Rev. Lett. **103**, 237601 (2009).
[6] F. Kagawa, M. Mochizuki, Y. Onose, H. Murakawa, Y. Kaneko, N. Furukawa, and Y. Tokura, Phys. Rev. Lett. **102**, 057604 (2009).
[7] T. Kimura, J. C. Lashley, and A. P. Ramirez, Phys. Rev. B **73**, 220401(R) (2006).
[8] S. Kanetsuki, S. Mitsuda, T. Nakajima, D. Anazawa, H. A. Katori, and K. Prokes, J. Phys.: Condens. Matter **19**, 145244 (2007).
[9] S. Seki, Y. Yamasaki, Y. Shiomi, S. Iguchi, Y. Onose, and Y. Tokura, Phys. Rev. B **75**, 100403(R) (2007).
[10] N. Terada, T. Nakajima, S. Mitsuda, H. Kitazawa, K. Kaneko, and N. Metoki, Phys. Rev. B **78**, 014101 (2008).
[11] E. Pachoud, C. Martina, B. Kundys, C. Simona, and A. Maignana, J. Solid State Chem. **183**, 344 (2010).
[12] T. Nakajima *et al.*, Phys. Rev. B **79**, 214423 (2009).
[13] T. Nakajima, S. Mitsuda, K. Takahashi, Y. Kaneko, T. Ito, M. Fukunaga, H. Kimura, and Y. Noda, J. Phys.: Conf. Ser. **200**, 012139 (2010).
[14] T. R. Zhao, M. Hasegawa, and H. Takei, J. Cryst. Growth **166**, 408 (1996).
[15] M. Blume, Phys. Rev. **130**, 1670 (1963).
[16] The orientations of the magnetic domains are not changed through the PD to FE-ICM phase transition because those are determined by the trigonal to monoclinic structural transition at ~10 K (Ref. 28).
[17] Effect of imperfect beam polarization of the incident neutrons has been corrected by subtracting the diffraction profile measured when the flipper is on (off) multiplied by $(1-p_0)/2$, where p_0 is the incident beam polarization, from the profile measured when the flipper is off (on).
[18] D. P. Belanger, A. R. King, and V. Jaccarino, Phys. Rev. B **31**, 4538 (1985).
[19] O. A. Petrenko, M. R. Lees, G. Balakrishnan, S. de Brion, and G. Chouteau, J. Phys.: Condens. Matter **17**, 2741 (2005).

[20] F. Ye, J. A. Fernandez-Baca, R. S. Fishman, Y. Ren, H. J. Kang, Y. Qiu, and T. Kimura, Phys. Rev. Lett. **99**, 157201 (2007).
[21] D. Meier, M. Maringer, T. Lottermoser, P. Becker, L. Bohaty, and M. Fiebig, Phys. Rev. Lett. **102**, 107202 (2009).
[22] Y. Yamasaki, H. Sagayama, T. Goto, M. Matsuura, K. Hirota, T. Arima, and Y. Tokura, Phys. Rev. Lett. **98**, 147204 (2007).
[23] H. Sagayama, K. Taniguchi, N. Abe, T. H. Arima, M. Soda, M. Matsuura, and K. Hirota, Phys. Rev. B **77**, 220407(R) (2008).
[24] T. Finger, D. Senff, K. Schmalzl, W. Schmidt, L. P. Regnault, P. Becker, L. Bohaty, and M. Braden, Phys. Rev. B **81**, 054430 (2010).
[25] P. G. Radaelli, L. C. Chapon, A. Daoud-Aladine, C. Vecchini, P. J. Brown, T. Chatterji, S. Park, and S.-W. Cheong, Phys. Rev. Lett. **101**, 067205 (2008).
[26] Spatial distribution of the wave number q due to macroscopic inhomogeneity of Al^{3+}-concentration might be another reason for the fact that the diffraction profiles in the ferroelectric phase are broad (Ref. 12). However, the E_p dependences of their widths are ascribed only to the changes in the average domain sizes, because no E_p dependences of q has been found in this system.
[27] K. Momma and F. Izumi, J. Appl. Crystallogr. **41**, 653 (2008).
[28] T. Nakajima, S. Mitsuda, T. Inami, N. Terada, H. Ohsumi, K. Prokes, and A. Podlesnyak, Phys. Rev. B **78**, 024106 (2008).